Vol. 423: 101–115, 2011
doi: 10.3354/meps08953

MARINE ECOLOGY PROGRESS SERIES
Mar Ecol Prog Ser

Published February 10

Growth rate and age distribution of deep-sea black corals in the Gulf of Mexico

N. G. Prouty[1,*], E. B. Roark[2], N. A. Buster[3], S. W. Ross[4]

[1]US Geological Survey, 400 Natural Bridges Drive, Santa Cruz, California 95060, USA
[2]Department of Geography, Texas A&M University, College Station, Texas 77843, USA
[3]US Geological Survey, 600 Fourth Street South, St Petersburg, Florida 33701, USA
[4]University of North Carolina at Wilmington, Center for Marine Science, 5600 Marvin Moss Ln, Wilmington, North Carolina 28409, USA

ABSTRACT: Black corals (order Antipatharia) are important long-lived, habitat-forming, sessile, benthic suspension feeders that are found in all oceans and are usually found in water depths greater than 30 m. Deep-water black corals are some of the slowest-growing, longest-lived deep-sea corals known. Previous age dating of a limited number of black coral samples in the Gulf of Mexico focused on extrapolated ages and growth rates based on skeletal ^{210}Pb dating. Our results greatly expand the age and growth rate data of black corals from the Gulf of Mexico. Radiocarbon analysis of the oldest *Leiopathes* sp. specimen from the upper De Soto Slope at 300 m water depth indicates that these animals have been growing continuously for at least the last 2 millennia, with growth rates ranging from 8 to 22 µm yr^{-1}. Visual growth ring counts based on scanning electron microscopy images were in good agreement with the ^{14}C-derived ages, suggestive of annual ring formation. The presence of bomb-derived ^{14}C in the outermost samples confirms sinking particulate organic matter as the dominant carbon source and suggests a link between the deep-sea and surface ocean. There was a high degree of reproducibility found between multiple discs cut from the base of each specimen, as well as within duplicate subsamples. Robust ^{14}C-derived chronologies and known surface ocean ^{14}C reservoir age constraints in the Gulf of Mexico provided reliable calendar ages with future application to the development of proxy records.

KEY WORDS: Black corals · Radiocarbon age · Growth rates · Gulf of Mexico · Oil spill

INTRODUCTION

Deep-sea coral (DSC) ecosystems are now widely recognized as biodiversity hotspots consisting of a large number of different mega- and macrofauna species (Roberts et al. 2009). These ecosystems provide habitat and reproductive grounds for certain commercially important fish species. Recent research expeditions conducted over the last decade have provided considerable new information on the distribution, habitat, and biodiversity of the DSC communities in the Gulf of Mexico (see review by Brooke & Schroeder 2007). The most extensive *Lophelia pertusa* habitat in the Gulf of Mexico is situated within the Bureau of Ocean Energy Management, Regulation and Enforcement (BOEMRE) lease block Viosca Knoll 826 (VK826) and has been the focus of several recent studies (Becker et al. 2005, Schroeder et al. 2005, CSA 2007, Cordes et al. 2008, Sulak et al. 2008).

We present radiocarbon (^{14}C) ages and growth rates from deep-water black corals (*Leiopathes* sp.) collected in the Gulf of Mexico along the continental slope at approximately 300 m water depth (Fig. 1). Information on growth rates and life spans of deep-sea corals is essential for conservation and management and for assessing the vulnerability of these organisms to both natural and anthropogenic perturbations. Black corals, in particular *Leiopathes* sp., are some of the slowest-

*Email: nprouty@usgs.gov

growing deep-sea corals relative to some other species (Newton & Bak 1979, Oakley 1988) and exhibit extreme longevities. For example, Roark et al. (2009) dated a *Leiopathes* sp. specimen from Hawaii to be 4265 ± 44 calendar yr (cal yr), with a radial growth rate of less than 5 µm yr^{-1}. A combination of factors such as low frequency of recruitment events, delayed first reproduction, limited larval dispersal, and the demonstrated longevity and slow growth rates suggest that it may take centuries for these species to recover from negative impacts. Longevity seems to be the key factor for population maintenance given the limited and complex genetic flow among black coral populations over long distances, as inferred by molecular markers (Miller 1997, 1998, Miller et al. 2010). Consequently, overexploitation of black corals without proper management could easily lead to local population extinction.

Previous age dating in the Gulf of Mexico focused on extrapolated ages and growth rates based on skeletal ^{210}Pb dating from a limited set of samples (Williams et al. 2006). Using both 'bomb-'produced radiocarbon over the last ~60 yr and conventional ^{14}C ages (based on the known radioactive decay rate) calibrated with reservoir corrections into calendar ages, robust and reliable ages, as well as growth rates, can be calculated (Roark et al. 2005, 2006, 2009, Sherwood et al. 2005). Here we performed radiocarbon measurements on samples selected from 2 distinct sites, Viosca Knoll and the head of De Soto Canyon (Fig. 1). In addition, multiple discs were cut from the base of each specimen and analyzed to investigate inter- and intra-sample reproducibility.

Black corals are colonial cnidarians in the order Antipatharia and are found in all oceans, usually in waters greater than 30 m deep (Grigg 1965). Black corals are long-lived, habitat-forming, sessile, benthic, suspension feeders (Grigg 1965, Lewis 1978, Parrish et al. 2002). Dense populations of these corals have been found in both the tropical western Atlantic and southwestern Pacific (e.g. Warner 1981, Grange 1985, Sánchez 1999). Six families are recognized (Opresko

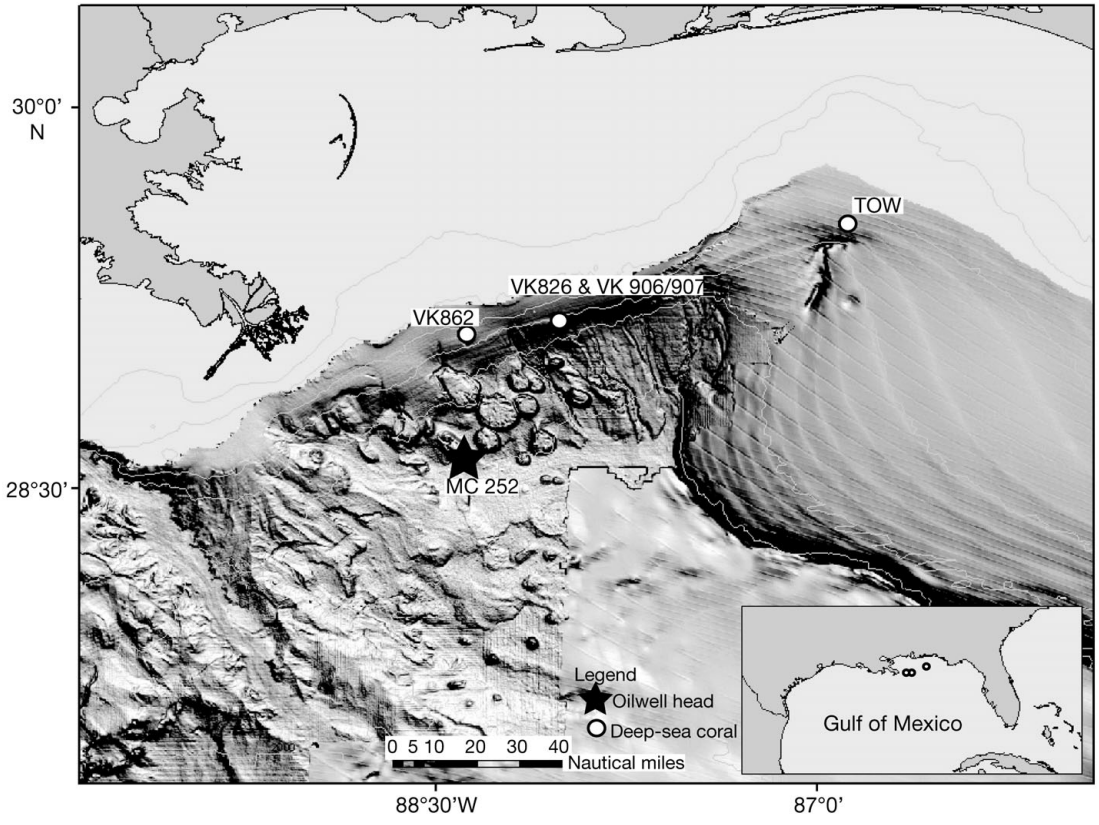

Fig. 1. Deep-sea coral sites were occupied between 2003 and 2009 to collect *Leiopathes* sp. from 2 different sites on the upper De Soto Slope subprovince: the head of De Soto Canyon and Viosca Knoll (VK), including the BOEMRE lease blocks VK862 and VK 906/907. The 'Deepwater Horizon' oil wellhead at the Mississippi Canyon, lease block MC252 (star), and the VK826 site are also marked. Tow samples collected by a trawl net are marked (TOW), while samples from the Viosca Knoll region were collected by the manned submersible, 'Johnson-Sea-Link', (JSL). All samples were collected at water depths of approximately 300 m

2001, 2002, 2003, 2004), and at least 20 species of antipatharians have been documented within the Gulf of Mexico region (Brooke & Schroeder 2007). At the VK 862-906/907 sites, at least 4 species of antipatharians were identified, making up one of the largest megafauna taxa at the sites (Sulak et al. 2008). Black corals are protected by international treaties and are listed in Appendix II of the Convention on International Trade in Endangered Species (CITES), restricting their exportation/importation.

Skeletons of black corals are comprised mainly of organic matter, consisting of successive layers of chitin and protein microlayers glued together by an organic cement layer (Goldberg 1991). The protein content accounts for almost 50%, while the chitin content is about 10 to 15% of the skeletal weight but can vary according to species (Goldberg et al. 1994). More recently, Nowak et al. (2009) found the chitin content to contribute between 6 and 18% and proteins and carbohydrates accounting for the remaining mass. The black coral skeleton is hard and sturdy and stands upright off the ocean floor. The architectural and mechanical properties of the black coral skeleton contribute to its stiffness (Kim et al. 1992).

Earlier studies have suggested that *Lophelia* sp., the scleractinian framework reef-building corals, are in part feeding on a food chain supported by chemosynthetic bacteria reliant on gas seeps (Hovland 1990). However, more recent isotopic studies have shown that methanotrophy is not a significant source of carbon for deep-sea coral reefs (Duineveld et al. 2004, Kiriakoulakis et al. 2004, Becker et al. 2009). Instead, these organisms acquire their carbon from surface-water organic matter after rapid transport to depth. The different organic carbon sources used by proteinaceous corals, viz. sedimentary, particulate, and dissolved organic carbon, were first investigated by Druffel et al. (1995) in *Gerardia* samples from the Straits of Florida using radiocarbon measured in the skeletal tips. According to isotopic mass balance calculations, the elevated post-bomb $\Delta^{14}C$ values (105‰) strongly suggested a surface-derived food source (i.e. particulate organic carbon) rather than sedimentary or dissolved organic carbon. More recently, studies have shown similarities between surface water $\Delta^{14}C$ derived from shallow-water coral $\Delta^{14}C$ records and deep-water black coral $\Delta^{14}C$ records (Roark et al. 2006, 2009, present study), highlighting the fact that these animals are acquiring their carbon from surface-water particulate organic matter (POM). These studies also show that the ^{14}C-derived age estimates of black corals are unaffected by feeding upon old resuspended sedimentary carbon (Roark et al. 2009).

MATERIALS AND METHODS

Sample sites. The samples for this study were collected from the Gulf of Mexico in 2003, 2004, 2005, and 2009 as part of several ongoing deep-sea coral ecosystem studies (e.g. CSA 2007, Sulak et al. 2008). Corals were collected from 2 different locations: the head of De Soto Canyon and Viosca Knoll, both east of the Mississippi Delta (Fig. 1, Table 1). In the Viosca Knoll region, 2 mound features were identified in lease blocks VK862 and VK906/907. These sites were of interest because of the extensive development of the coral *Lophelia pertusa* in the Viosca Knoll region (Brooke & Schroeder 2007, Sulak et al. 2008). As described by Sulak et al. (2008), the substrate capping the topographic mound features at these sites consisted of extensive deposits of authigenic goethite, a ferric oxide mineral, providing a substrate for settlement. The samples from the head of De Soto Canyon were inadvertently collected by bottom trawl, resulting in little information regarding their exact location. In comparison, Davies et al. (2010) provided a more detailed description of Viosca Knoll (VK826), which is located approximately 37 km east–northwest of VK862-906/907. Several key findings of their study include documentation of relatively low dissolved oxygen concentrations (27 to 28 ml l^{-1}) and a 24 h diel vertical migration of zooplankton that was suggested to form part of the food chain for the corals. Sediment trap

Table 1. *Leiopathes* sp. Sample ID and location for specimens collected between 2003 and 2009 within the Gulf of Mexico from 2 different sites on the upper De Soto Slope subprovince, viz. the head of De Soto Canyon (archived at the US National Museum) and Viosca Knoll. Sample IDs include information about whether the samples were collected by trawl (TOW) or manned submersible, the 'Johnson-Sea-Link' (JSL). Dates are given as mm/dd/yy

Sample ID	Collection date	Site	Latitude (N)	Longitude (W)	Depth (m)
GOM-TOW-BC1	11/15/03	De Soto Canyon	29° 32.24′	86° 52.19′	304
GOM-TOW-BC2	11/15/03	De Soto Canyon	29° 32.24′	86° 52.19′	304
GOM-JSL05-4876-BC1	9/17/05	Viosca Knoll 906/907	29° 04.39′	87° 37.22′	312
GOM-JSL09-3728-BC1	9/20/09	Viosca Knoll 862	29° 06.41′	88° 23.10′	317
GOM-JSL04-4734-BC1	7/23/04	Viosca Knoll 862	29° 06.22′	88° 23.05′	310

data consisted of fine-grained aggregates of riverine origin with particles of high organic carbon content (Davies et al. 2010).

Sample collection. On 15 November 2003, a bottom trawl inadvertently collected 3 specimens of living black coral, which are archived at the US National Museum (USNM), from the head of DeSoto Canyon at a depth of 304 m (Table 1). Two of these specimens were used in this study. The manned submersible 'Johnson-Sea-Link' (JSL, Harbor Branch Oceanographic Institute), was used to collect live black coral colonies from the Viosca Knoll sites at depths of 310 to 317 m (Table 1). Specimens archived at the USNM were tentatively identified based on branch pattern and size (D. Opresko pers. comm.) as *Leiopathes* sp. Species identification of the remaining samples was done at the time of collection and confirmed by comparisons with previously identified black corals. After collection, tissues were removed with forceps, and the specimens were rinsed in fresh water and air-dried on deck. The objective of the project was to calculate long-term growth rates and ages; therefore, samples with basal diameters >2 cm appropriate for measuring long-term growth rates and ages were selected for radiocarbon analysis. The age range of specimens discussed below is a function of the variability in samples collected and the natural distribution of ages at a given site.

Sample preparation. Cross-sectional discs ~0.3 to 0.5 cm thick were cut from the basal portion of the corals using a diamond band saw. Thin sections ~30 and 100 µm thick were prepared commercially for scanning electron and petrographic imaging. Following Williams et al. (2006, 2007), growth bands were separated by placing the discs in a solution of 4 g of potassium hydroxide (KOH) in 50 ml of water for ~1 wk. KOH acts as an effective protein denaturant and solvent causing the skeleton to swell and growth band laminae to separate, in a similar fashion to concentrated formic acid treatment (Goldberg 1991). This treatment does not appear to have any effect on the isotopic composition of the skeleton (Williams 2009) and was confirmed by replicate radiocarbon dates from samples treated with KOH versus samples that were microdrilled without any chemical band separation. Using forceps and a reflected-light microscope, individual growth bands were separated, rinsed with Milli-Q water, and dried overnight. Depending on the size of the disc and the ease of growth band separation, this yielded a maximum of 325 and a minimum of 66 subsamples. Typically, individual bands were between 100 and 200 µm thick as measured by a dial and digital caliper. A small subset of samples was also drilled from the center (inner), middle, and outer portions across the radial transects using a hand-held microdrill.

Visual ring counts. In preparation for scanning electron microscope (SEM) analysis, samples were impregnated with epoxy, and 100 µm thin sections were prepared commercially and imaged at the SEM facility at the University of South Florida, St Petersburg, Florida (Fig. 2a). Visual ring counts were conducted on the SEM images by counting the optically visible light lines (Fig. 2b,c). The dark bands visible in Fig. 2 represent organic cement layers that serve to 'glue' the growth laminae together (Goldberg 1991, Nowak et al. 2009). In contrast to Goldberg's (1991) observation that the skeleton of *Antipathes fiordensis* is composed of concentric laminae interspersed by radially oriented spines, we did not observe spines in the SEM images of the *Leiopathes* specimens; therefore, they did not interfere with the visual growth ring counts. Visual ring counts were also determined by creating a grayscale series using the SEM image and ImageJ software (Abramoff et al. 2004). Each visible light band was counted regardless of its thickness. For each method, the reported ring counts were determined by taking the average and standard deviation of 5 independent traverses.

Analytical measurements. Subsamples between 1 and 6 mg, depending on laboratory requirements, were prepared for Accelerator Mass Spectrometry (AMS) radiocarbon (^{14}C) dating at the following centers: The Center for Accelerator Mass Spectrometry, Lawrence Livermore National Laboratory (CAMS); The Keck Carbon Cycle AMS laboratory at UC Irvine (KCCAMS); The National Ocean Sciences Accelerator Mass Spectrometry Facility (NOSAMS); and Beta Analytic. Samples were pretreated either with a deionized (DI) water rinse 3 times or a weak hydrochloric acid (1 N) rinse, placed on a hot plate for 20 min, and then rinsed 3 times with DI. Excess liquid was pipetted off prior to drying down on the hot plate. The carbon in the samples was converted to CO_2 via sealed-tube combustion with silver and CuO, and upon cyrogenic purification, the CO_2 was reduced to graphite in the presence of iron catalyst and a stoichiometric excess of hydrogen. Process blanks included either a coal or calcite blank.

Post-bomb chronology. The $D^{14}C$ values (i.e. radiocarbon values without age correction) were age corrected to account for decay that took place between collection (or death) and the time of measurement using the following equation: $\Delta^{14}C = ([Fm \times \text{age correction}] - 1) \times 1000$, where Fm is fraction modern (modern is 1950 AD) and age correction is defined as exp(1950 – year of measurement)/8267) (Stuiver & Polach 1977). Radiocarbon results are reported as $\Delta^{14}C$ (‰) and conventional radiocarbon age (CRA) after applying a $\delta^{13}C$ correction (Stuiver & Polach 1977). Analytical uncertainty was 1.3 to 3.9‰, and age errors ranged between

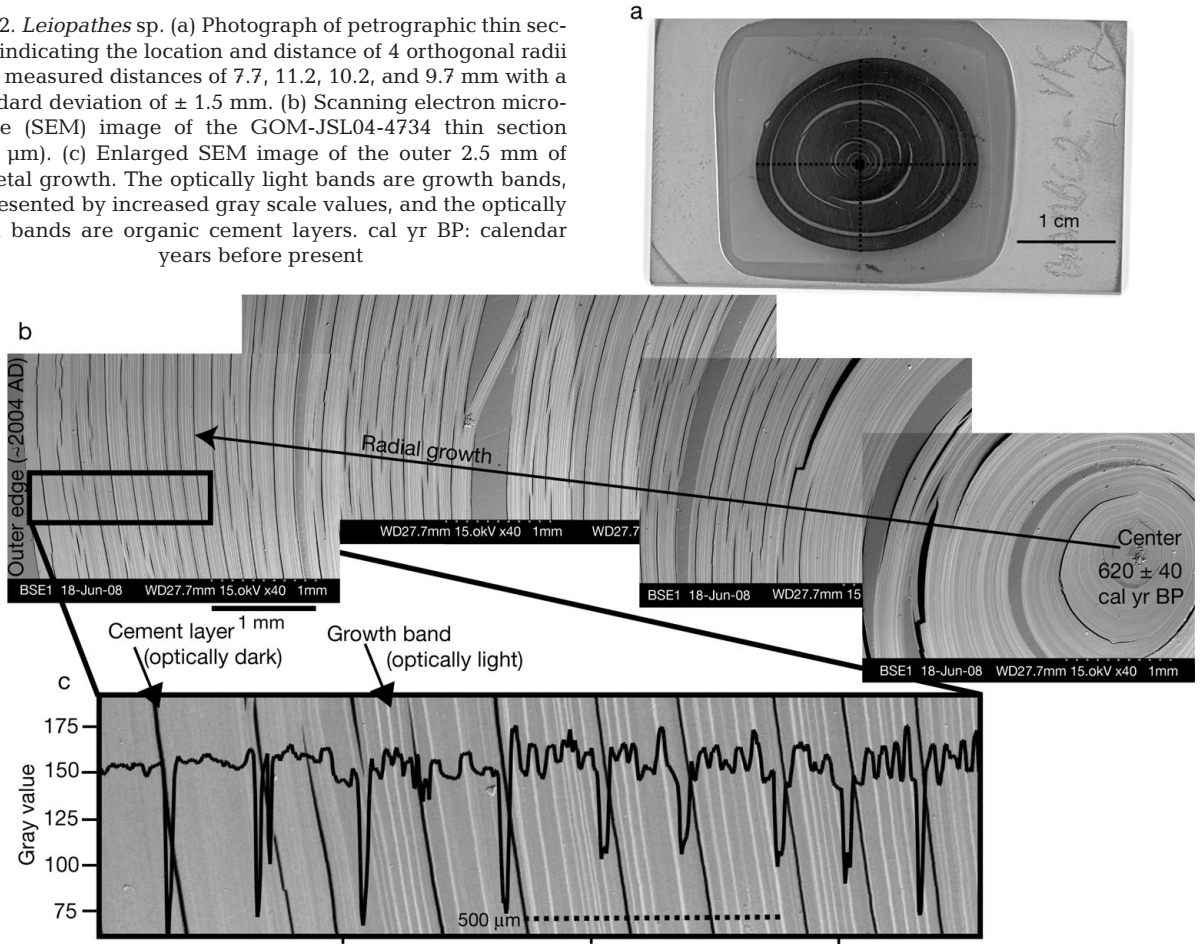

Fig. 2. *Leiopathes* sp. (a) Photograph of petrographic thin section indicating the location and distance of 4 orthogonal radii with measured distances of 7.7, 11.2, 10.2, and 9.7 mm with a standard deviation of ± 1.5 mm. (b) Scanning electron microscope (SEM) image of the GOM-JSL04-4734 thin section (100 µm). (c) Enlarged SEM image of the outer 2.5 mm of skeletal growth. The optically light bands are growth bands, represented by increased gray scale values, and the optically dark bands are organic cement layers. cal yr BP: calendar years before present

±15 and 40 yr. Conventional ^{14}C ages were converted to cal yr using a reservoir correction (ΔR) of 240 ± 13 yr (ΔR of −30 ± 26 ^{14}C yr) based on pre-bomb surface water radiocarbon measurements derived from a coral record from the Flower Garden Banks, northern Gulf of Mexico (Wagner et al. 2009) and the Calib 6.0 program (Stuiver & Reimer 1993). Both the reported radiocarbon and calibrated age uncertainties are reported at the 1 sigma level.

For those samples too young to apply a CRA, the chronology was developed using the bomb-derived ^{14}C age model based on otolith and shallow coral $\Delta^{14}C$ values. In the Gulf of Mexico, the bomb-derived ^{14}C was constructed using the bomb $\Delta^{14}C$ curve from the otolith and shallow coral $\Delta^{14}C$ curves (Baker & Wilson 2001, Wagner 2009). The rising limb of the bomb-^{14}C curve from these data sets represents $\Delta^{14}C$ data from 1955 to 1997 (n = 25), and the descending limb represents $\Delta^{14}C$ data from 1975 to 1996 (n = 12). The age models prior and subsequent to the bomb peak are linear, with regression coefficients of 0.92 and 0.97, respectively (Fig. 3). The bomb-$\Delta^{14}C$ curve is a reflection of artificially produced ^{14}C from detonation of nuclear test weapons in the atmosphere in the late 1950s and early 1960s. The peak in surface ocean ^{14}C occurs ~10 yr after the atmospheric peak due to result of air–sea ^{14}C exchange and the ~decadal time delay for isotopic equilibration (Broecker & Peng 1982). From the atmospheric peak in 1963, the level of $^{14}CO_2$ has decreased exponentially with a mean life of about 16 yr, not due to radioactive decay, but due to mixing with large marine and terrestrial carbon reservoirs (e.g. Levin & Kromer 2004).

RESULTS

Radiocarbon age

CRAs were determined from 5 different specimens (Table 1), plus replicate samples on adjacent discs in 2 of the specimens (GOM-TOW-BC1 and GOM-TOW-BC2). Conventional ^{14}C ages were converted to calendar years before present (cal yr BP), and these results are presented in Table 2 and reported as the median probability age. The 1 sigma calibrated age ranges are re-

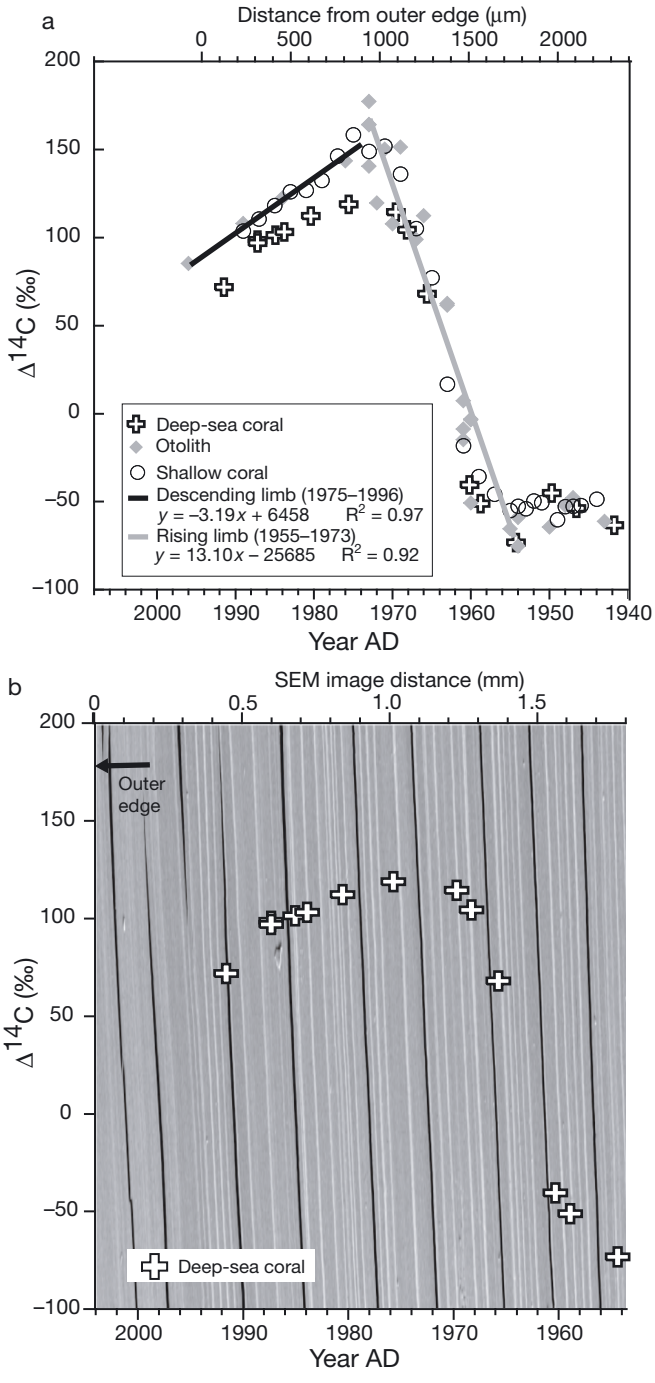

Fig. 3. (a) Bomb-derived $\Delta^{14}C$ (‰) from red snapper otoliths (n = 26; diamonds) in the Gulf of Mexico (Baker & Wilson 2001) and shallow coral $\Delta^{14}C$ values (n = 27; circles) from the Flower Garden Banks (Wagner 2009) from 1943 to 1996. Superimposed on the reference curves is the deep-sea antipatharian *Leiopathes* sp. coral $\Delta^{14}C$ record (crosses) from the GOM-JSL04-4734-BC1 specimen versus distance from outer edge (µm). An age model was constructed from the combined otolith and shallow water coral data to yield an equation for the rising limb (1955–1997) and the descending limb (1975–1996) of the bomb-^{14}C curve. The $\Delta^{14}C$ analytical uncertainty was 1.3 to 3.9‰. (b) *Leiopathes* sp. coral bomb-^{14}C curve superimposed on the enlarged scanning electron microscope image

ported in the Supplement at www.int-res.com/articles/suppl/m423p101_supp.pdf. The oldest specimen (GOM-JSL09-3728-BC1) was from Viosca Knoll (VK862). The center ^{14}C age of this specimen was 2380 ± 30 ^{14}C yr; the corresponding calibrated age was 2040 ± 40 cal yr BP (Table 2). Since this specimen was collected alive, the date of collection (2009) was used to calculate the life span, calculated as the difference between the inner calendar year and the date of collection, yielding 2100 ± 40 yr. As discussed below, the bomb-derived ^{14}C age model based on otolith and shallow coral $\Delta^{14}C$ values and the bomb-derived ^{14}C detected in the outermost portion of this specimen can be used to estimate an age for the outermost portion of the skeleton. This is useful when it is not known if the specimen was collected alive. In this specimen, the outermost $\Delta^{14}C$ value (53‰) corresponds to an age of 2003 yr AD, yielding a life span of 2090 ± 40 yr (center age of 2040 ± 40 cal yr BP or 90 cal yr BC).

The second oldest specimen was collected from the head of De Soto Canyon (GOM-TOW-BC2), with maximum center age dates between 2100 ± 40 and 2030 ± 15 ^{14}C yr, reflecting radiocarbon analysis from discreetly milled and delaminated samples, respectively (Table 3). The reservoir corrected calibrated ages are 1720 ± 50 cal yr BP and 1630 ± 30 cal yr BP. Accounting for the ^{14}C age errors (± 30 to 50 yr), the minimum age differences from these replicate analyses, which were conducted at different laboratories on 2 adjacent discs using different subsampling techniques, is within 10 yr of the ^{14}C age. The outermost sample from the GOM-TOW-BC2 disc that was discreetly drilled did not indicate the presence of bomb-^{14}C (–49‰). This was because the outermost layer, sampled at ~0.6 mm resolution, integrated ~75 yr of growth, including years in which no bomb carbon was produced. In comparison, the outermost layer (~200 µm thick) from an adjacent disc that was delaminated yielded bomb-^{14}C (47‰; Table 3). Using the bomb-derived ^{14}C age model based on otolith and shallow coral $\Delta^{14}C$ values (see 'Discussion'), we determined that the outermost $\Delta^{14}C$ values corresponded to an age of 1964 yr AD, and the resultant life span of this sample was approximately 1640 ± 30 yr. In comparison, using the difference between the date of collection (2003) and the inner ^{14}C age, we determined that the life span was 1680 ± 30 yr.

Specimen GOM-TOW-BC1 collected from the De Soto Canyon was age dated between 1090 ± 35 and 1080 ± 25 ^{14}C yr, reflecting radiocarbon analysis from discreetly milled and delaminated samples, respectively (Table 3). Reservoir corrected age dates yielded center ages between 680 ± 45 and 670 ± 35 cal yr BP (Table 2). Unlike specimen GOM-TOW-BC2, there was no bomb-^{14}C detected in the outermost skeletal samples in either disc from the GOM-TOW-BC1 specimen (Tables 3 & 4). The outermost replicated samples

Table 2. *Leiopathes* sp. Conventional ^{14}C ages were converted to calendar years before present (cal yr BP) using a reservoir correction (ΔR) of 240 ± 13 yr (ΔR of −30 ± 26 ^{14}C years) based on pre-bomb surface water radiocarbon measurements derived from a coral record from the Flower Garden Banks, northern Gulf of Mexico (Wagner et al. 2009), and the Calib v6 program (Stuiver & Reimer 1993). Calendar years BP are reported as median probability age. See the Supplement at www.int-res.com/articles/suppl/m423p101_supp.pdf for 1 sigma calibrated age ranges. Age errors ranged between ± 30 and 65 yr. The life spans were calculated as the difference between the inner calendar year and the date of collection, unless the outer sample did not contain modern ^{14}C, in which case the difference in ^{14}C age was used. Growth rates in parentheses indicate rates calculated on adjacent discs from microdrilling an outer, middle, and inner sample. Regression coefficients are listed for the linear-age models

Sample	^{14}C age inner	Cal yr BP	^{14}C age outer	Growth rate (μm yr^{-1})	R^2	Life span (yr)
GOM-TOW-BC1	1080 ± 25	670 ± 36	550 ± 60	22 (21)	0.46	530
GOM-TOW-BC2	2030 ± 15	1630 ± 30	Modern	8 (8)	0.97	1680
GOM-JSL04-4734-BC1	1020 ± 30	620 ± 40	Modern	17	0.85	670
GOM-JSL05-4876-BC1	1260 ± 30	830 ± 40	Modern	14	0.96	890
GOM-JSL09-3728-BC1	2380 ± 30	2040 ± 40	Modern	8	0.87	2100

Table 3. *Leiopathes* sp. Replicate studies were conducted for radiocarbon analysis on adjacent discs using different subsampling techniques (microdrilling and chemical band separation) at different Accelerator Mass Spectrometry laboratories ([a]Lawrence Livermore National Laboratory, LLNL; [b]Beta Analytic; [c]University of California Irvine). Analytical uncertainty for $\Delta^{14}C$ was 1.3 to 3.9‰. Those sample analyzed at LLNL were subsampled by microdrilling an inner, middle, and outer sample, whereas the remaining samples were chemically separated using potassium hydroxide (KOH)

Sample	^{14}C age inner	^{14}C age outer	Outer $\Delta^{14}C$ (‰)	Inner $\Delta^{14}C$ (‰)	No. samples
GOM-TOW-BC1[a]	1090 ± 35	550 ± 35	−73 ± 3.9	−133 ± 3.4	3
GOM-TOW-BC1[b]	1080 ± 25	550 ± 60	−73 ± 3.5	−132 ± 2.7	35
GOM-TOW-BC2[c]	2030 ± 1 5	Modern	47 ± 1.8	−229 ± 1.3	12
GOM-TOW-BC2[a]	2100 ± 40	350 ± 30	−49 ± 3.3	−235 ± 3.5	3

yielded equivalent ages, 550 ± 35 and 550 ± 60 ^{14}C yr. The reservoir-corrected calibrated ages are 210 ± 45 and 205 ± 65 cal yr BP. According to the inner and outer ^{14}C ages from the delaminated samples, this specimen had a life span of approximately 530 ± 60 yr.

The 2 remaining samples were collected from separate sites on Viosca Knoll ~1100 m apart and occupied the same depth horizon, centered at 325 m (Sulak et al. 2007). The center age of GOM-JSL04-4734-BC1 was dated at 1020 ± 30 ^{14}C yr (620 ± 40 cal yr BP; Table 2). The outermost 1.5 mm contained bomb-derived ^{14}C (72‰; Table 4). The post-bomb age model suggests that the life span of this sample from Viosca Knoll is approximately 670 ± 40 yr, with the outermost sample representing growth in the year 1997 (Fig. 3). Incorporating the date of collection (2004) yielded a life span of 670 ± 40 yr. In comparison, radiocarbon analysis of GOM-JSL05-4876-BC1 yielded a center age of 1260 ± 30 ^{14}C yr (830 ± 40 cal yr BP; Table 2). The outermost sample contained bomb-derived ^{14}C (69‰; Table 4), corresponding to an age of 1998 AD according to the post-bomb age model and yielding a life span of approximately 870 ± 40 yr, or 890 ± 40 yr given that the specimen was collected alive in 2005.

Table 4. *Leiopathes* sp. Bomb-derived ^{14}C (defined as those values above a pre-bomb mean of −50‰) was found in all specimens except GOM-TOW-BC1. Analytical uncertainty for $\Delta^{14}C$ was ±1.3 to 3.9‰. The reported radius represents the mean of 4 orthogonal radii measured on each disc with a standard deviation of between 1 and 2 mm. Radiocarbon analysis was conducted at different Accelerator Mass Spectrometry laboratories ([a]University of California Irvine; [b]Beta Analytic; [c]National Ocean Sciences Accelerator Mass Spectrometry Facility)

Sample	Outer $\Delta^{14}C$ (‰)	Inner $\Delta^{14}C$ (‰)	No. samples	Radius (mm)
GOM-TOW-BC1[b]	−73 ± 3.5	−132 ± 2.7	35	7.6
GOM-TOW-BC2[a]	47 ± 1.8	−229 ± 1.3	12	11.4
GOM-JSL04-4734-BC1[b,c]	72 ± 3.6	−126 ± 3.1	48	8.8
GOM-JSL05-4876-BC1[a]	69 ± 3.6	−151 ± 2.8	10	14.3
GOM-JSL09-3728-BC1[a]	53 ± 3.5	−261 ± 2.5	11	18.1

Growth rates

Radial growth rates were calculated by plotting reservoir corrected ^{14}C age (year AD) versus sample distance from the outer edge (μm; Fig. 4a–e). Samples from the head of De Soto Canyon exhibited linear growth rates of 8 to

22 µm yr^{-1}, with the older sample (GOM-TOW-BC2) exhibiting a slower growth rate (Table 2). Average radii from GOM-TOW-BC2 adjacent discs were 15 and 11.1 mm and yielded equivalent growth rates of 8 µm yr^{-1}. Likewise, radii from GOM-TOW-BC1 discs were 9.7 and 7.6 mm and yielded growth rates of 21 and 22 µm yr^{-1}, respectively. The growth rates were strongly linear, with R^2 values between 0.85 and 0.97

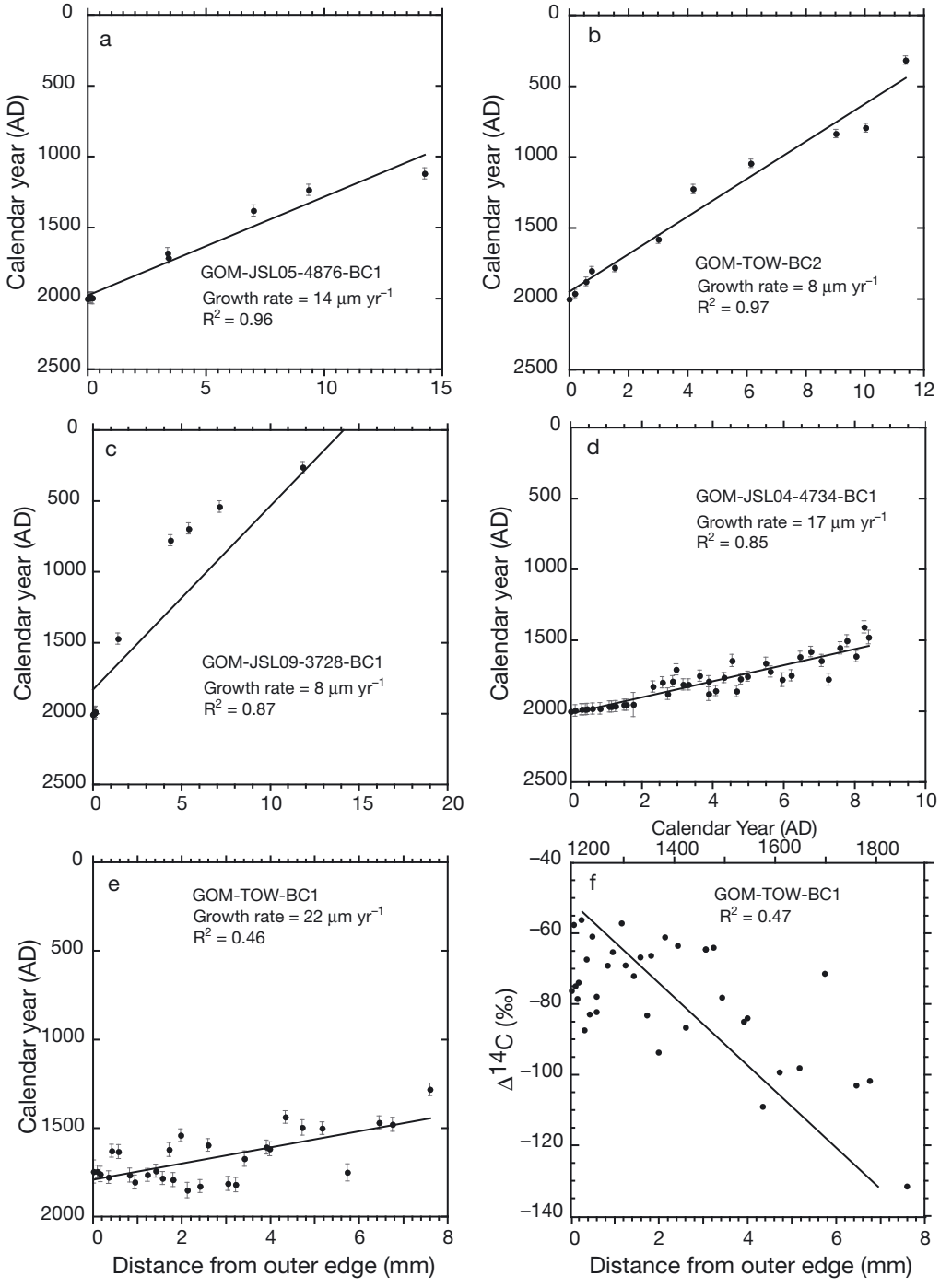

Fig. 4. *Leiopathes* sp. (a–c) Distance from outer edge (mm) versus reservoir-corrected calendar age (AD) for the 5 deep-sea black coral samples: (a) GOM-JSL05-4876-BC1, (b) GOM-TOW-BC2, (c) GOM-JSL09-3728-BC1, (d) GOM-JSL04-4734-BC1, (e) GOM-TOW-BC1). Radial growth rates were calculated as the slope of the linear regression line. Growth rates were strongly linear, with R^2 values between 0.85 and 0.97 (Table 2). One exception is the specimen GOM-TOW-BC1, with a correlation coefficient of 0.46 (panel e). (f) Radiocarbon ($\Delta^{14}C$) variability of GOM-TOW-BC1 versus distance from outer edge (mm) and calendar year (AD) with an analytical uncertainty of 1.3 to 3.9‰

(Table 2). One exception was the specimen GOM-TOW-BC1, with a correlation coefficient of 0.46 (n = 29). Approximately 30% of the data (10 samples) were outside the age error window with equal distribution both above and below this window (Fig. 4e), and there was no systematic pattern in the distribution of these outliers in this specimen (GOM-TOW-BC1). In summary, 5 samples yielded younger than expected ages, and 5 samples yielded ages older than expected according to the linear-age growth model. Replicate radiocarbon analysis was conducted on 2 of the outliers, 1 sample each from above and below the regression line. Both replicates yielded similar ^{14}C ages, 635 ± 30 and 595 ± 30, and 480 ± 30 and 480 ± 30 yr at sample distances of 578 and 3048 µm from the outer edge, respectively.

The growth rates for the Viosca Knoll samples ranged from 8 to 17 µm yr^{-1} (Table 2). At Viosca Knoll, the sample (GOM-JSL04-4734-BC1) with the shortest life span (670 ± 40 yr) also displayed the fastest growth rate of 17 µm yr^{-1} (R^2 = 0.85; Fig. 4d). With a radius of 14.3 mm, the GOM-JSL05-4876-BC1 sample from VK906/907 yielded a growth rate of 14 µm yr^{-1} (R^2 = 0.96; Fig. 4a). In comparison, the older and larger sample from VK862 (GOM-JSL09-3728-BC1), with a radius of 18.1 mm, yielded a slower growth rate (8 µm yr^{-1}, R^2 = 0.87; Fig. 4c). There was an inverse relationship between coral ages (defined as life span) versus growth rate at both sites (R^2 = 0.88; Fig. 5).

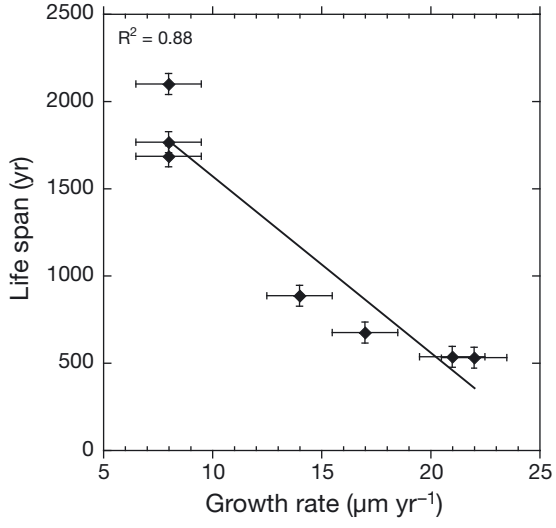

Fig. 5. *Leiopathes* sp. Life spans (calculated as the difference between the inner calendar year and the date of collection, unless the outer sample did not contain modern ^{14}C, in which case the difference in ^{14}C age was used) versus growth rate (µm yr^{-1}) calculated from black coral samples collected in the Gulf of Mexico. There is evidence of an inverse relationship between age (defined as life span) and growth rate at both sites (R^2 = 0.88). Error bars represent the life span uncertainty (± 60 yr) and growth rate uncertainty (1.5 µm yr^{-1})

The uncertainty of the estimated life spans and growth rates goes beyond just the uncertainty of the calibrated radiocarbon ages. By way of example, we calculated the uncertainty of the innermost calibrated radiocarbon age for the oldest specimen (GOM-JSL09-3728-BC1) by calculating the age differences of the median probability age from the minimum age (55 yr) and maximum ages (60 yr) of the calibrated age range (cal BP; see the Supplement at www.int-res.com/articles/suppl/m423p101_supp.pdf). For all samples, the largest age difference between the minimum age and maximum ages or the median probability age was ~120 yr while the average of all such age differences for all calibrated radiocarbon results was approximately 60 yr. For the age uncertainty of the outermost age, we presumed the worst-case scenario of not knowing whether the specimen was collected alive or dead and assigned a qualitative age uncertainty of ±5 yr based on the correlation of bomb-derived $\Delta^{14}C$ in the specimen to an age model constructed using the bomb $\Delta^{14}C$ curve from otolith and shallow coral $\Delta^{14}C$ curves (Baker & Wilson 2001, Wagner 2009; Fig. 3). Thus, using an uncertainty of ±5 yr for the outermost age and ±60 yr (or worst case ±120 yr for all the samples) and calculating the root mean squared error (RMSE) resulted in an uncertainty estimate of ±60 yr (worst case ±120 yr) for the life span. In calculating the uncertainty of the estimated growth rates, one must consider the estimated life span uncertainty along with the uncertainty of the radial distance measurement, which we qualitatively estimated at ±1 mm for the GOM-JSL09-3728-BC1 specimen with a radial distance of 18.1 mm. The estimated uncertainty of radial distance is purposely large in order to account for the asymmetry of the specimens and measurement error. By calculating the growth rate using minimum radial distance and maximum life span (17.1 mm per 2160 yr = 7.9 µm yr^{-1}) and comparing those results to growth rates calculated using maximum radial distance and minimum life span (19.1 mm per 2040 yr = 9.4 µm yr^{-1}), the resulting average growth rate estimate uncertainty will be on the order of ~ ±1.5 µm yr^{-1}. The results of this exercise show that life span differences greater than ±60 yr on average and growth rate difference greater than ±1.5 µm yr^{-1} are significant at the 1 sigma level.

Bomb radiocarbon and post-bomb age model

Bomb radiocarbon (values above a pre-bomb $\Delta^{14}C$ mean of −50‰) was found in all specimens except the GOM-TOW-BC1 sample (Table 4). The bomb-$\Delta^{14}C$ curve was captured in the GOM-JSL04-4734-BC1 $\Delta^{14}C$ record (Fig. 3). Pre-bomb baseline values centered at −56‰, with the first influx of bomb-derived ^{14}C at

1504 µm. Post-bomb $\Delta^{14}C$ values increased from –40 to 68‰ within 238 µm. Pre-bomb averages (1943 to 1955) from red snapper *Lutjanus campechanus* otoliths (n = 26) in the Gulf of Mexico (Baker & Wilson 2001) and shallow coral (*Montastraea faveolata*) $\Delta^{14}C$ values from the Flower Garden Banks (n = 27; Wagner et al. 2009) were –60 and –53‰, representative of pre-bomb surface ocean $\Delta^{14}C$ values. Bomb-^{14}C values peaked (119 ± 59‰) in the GOM-JSL04-4734-BC1 specimen at ~1000 µm (Fig. 3). In comparison, $\Delta^{14}C$ values from the otolith data peaked at 177 ± 91‰ in 1973 (Baker & Wilson 2001), and shallow coral $\Delta^{14}C$ values peaked at 158 ± 35‰ in 1975 (Wagner 2009). The deep-sea coral peak of 119‰ can be age-dated between 1973 and 1975. In the remaining outer skeletal samples (n = 5), representing the outer 600 µm, $\Delta^{14}C$ values decreased with the outermost sample yielding a $\Delta^{14}C$ value of 72 ± 36‰ at 125.3 µm. The growth rate during the bomb spike can be calculated using the local radiocarbon inflection point that is assigned a calendar year of 1957 and the bomb peak that is assigned a calendar year of 1975. With a collection date of 2003, growth rates were calculated over the following time intervals: 1957–1975, 1975–2003, and 1957–2003, yielding linear (R^2 = 0.99–0.98) growth rates of 41, 24, and 33 µm yr^{-1}, respectively. These growth rates over the outermost 1.5 mm are on average twice as fast as the growth rate calculated over the entire radius of the specimen (17 µm yr^{-1}). Despite displaying a faster growth rate over the outermost portion of growth, the average growth rate over the entire lifespan remained relatively linear (R^2 = 0.85; Fig. 4d, Table 2).

Bomb-derived ^{14}C from GOM-TOW-BC2 was only measured in the outermost delaminated sample (at a distance of 191 µm from the outer edge) with a $\Delta^{14}C$ value of 47 ± 18‰. According to the age model, this yielded an approximate date of 1964 yr AD. Although sampled at less than a 200 µm interval in the outer 1 mm, the remaining samples yielded pre-bomb $\Delta^{14}C$ values averaging –60‰. After ~1.5 mm from the outer edge, $\Delta^{14}C$ values decreased linearly with sample distance, indicative of radioactive decay. In contrast to the delaminated samples, the microdrilled samples did not yield bomb-derived ^{14}C. Instead, the outermost drilled sample yielded a $\Delta^{14}C$ value of –49 ± 33‰.

The outermost ~150 µm for the samples GOM-JSL05-4876-BC1 and GOM-JSL09-3728-BC1 were subsampled at a higher resolution (27 to 40 µm increments) for radiocarbon analysis in order to capture the bomb peak. For both samples, $\Delta^{14}C$ values decreased towards the outer edge; therefore, the age model based on the descending limb of the reference bomb-^{14}C chronology was used to assign calendar ages. Accordingly, the outermost ~150 µm for the samples GOM-JSL05-4876-BC1 and GOM-JSL09-3728-BC1 represented growth since 1996 and 1990 with dates of collection at 2005 and 2009, respectively. Accordingly, the growth rates over this period were 18 and 9 µm yr^{-1}. In comparison to post-bomb growth rates calculated from the GOM-JSL04-4734-BC1 specimen, the latter 2 samples from Viosca Knoll did not exhibit a doubling in growth rate during the most recent decades.

Band counting

Layer counting of sample GOM-JSL04-4734-BC1 based on an SEM image yielded an average age of 576 ± 37 yr compared to the calculated life span of 670 ± 40 yr, calculated as the difference between the reservoir corrected inner layer and date of collection. Taking into account the ^{14}C-age error (37 to 40 yr), there is a minimum age difference of 21 yr based on these 2 dating techniques. Visual ring counts in the outermost 1.77 mm (Fig. 2c) were also compared to the high-resolution chronology developed from the bomb-^{14}C curve derived from otolith and shallow coral $\Delta^{14}C$ values, as discussed below. According to this age model, the outermost skeletal growth in this specimen covered a time period of 49 yr (1955 to 2004; Fig. 3b). Excluding the outer 300 µm where the visual rings were indistinct, visual ring counts in the outermost 1.77 mm revealed approximately 55 ± 3 distinct bands (Fig. 2c). Therefore, the estimated age error between these 2 age estimates is between 3 and 9 yr.

DISCUSSION

Visual ring counts

Previous studies of growth ring structure in black corals indicated that the skeleton is formed of concentric coeval rings (Grange & Goldberg 1993), such that visually counting the rings provides a means of developing radial growth chronologies. For example, in shallow-water black corals from the Red Sea, Risk et al. (2009) found good correspondence between the number of visually counted rings and ages calculated using a bomb radiocarbon analysis compared to a local independent bomb curve. This approach has also been applied to gorgonian corals (Risk et al. 2002, Sherwood et al. 2005). In our study, visual ring counts of GOM-JSL04-4734-BC1 based on SEM images yielded an average age of 576 ± 37 yr compared to the calculated life span of 670 ± 40 yr. The minimum age difference between these 2 age calculations is 17 yr. Given a growth rate of 17 µm yr^{-1}, this age difference represents ~0.30 mm of skeletal growth. While black corals

display radial growth, the growth is not necessarily symmetrical. In other words, the core can be off-center. For example, the standard deviation on orthogonal radii was ±1.5 mm for the GOM-JSL04-4734-BC1 specimen (Fig. 2a). Therefore, the distance equivalent to calculated age difference (i.e. 0.30 mm) is within the variance associated with the growth asymmetry. Visual ring counting therefore appears to be a viable approach for aging black corals from the Gulf of Mexico. This observation is further validated by a strong similarity in ages based on visual ring counts in this specimen to the bomb-derived ^{14}C age models. The estimated age error between the 2 approaches, 3 to 9 yr, suggests annual ring formation. Annual variations in food supply and surface productivity may be factors influencing annual skeletal growth layers (Sherwood 2002); however, the exact mechanism to explain annual growth formation remains unclear. While results from our study support the notion of annual growth rings as suggested by Williams et al. (2007) in black coral samples from the southeastern US, further studies are required to validate this assumption.

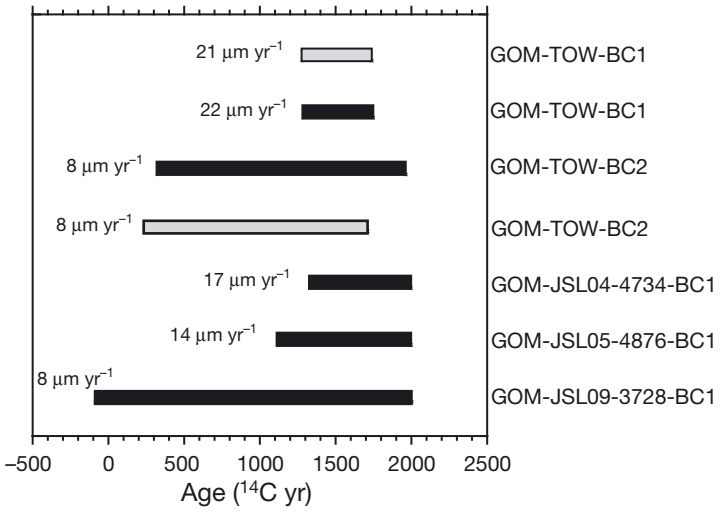

Fig. 6. *Leiopathes* sp. Life span and growth rate distribution of black coral collected from sites (~300 m) on the upper De Soto Slope subprovince, Gulf of Mexico. Conventional radiocarbon ages were determined from 5 different specimens including replicate samples on adjacent discs in 2 of the samples (GOM-TOW-BC1 and GOM-TOW-BC2), as indicated by gray bars. These data indicate that these animals have been growing continuously for at least the last 2 millennia, with growth rates ranging from 8 to 22 µm yr^{-1}

Radiocarbon dating

The reliability of ^{14}C age dating was investigated by conducting radiocarbon analysis on adjacent discs as well as running replicates of individually delaminated samples. The high degree of reproducibility found between discs as well as within duplicate subsamples highlights the robustness of ^{14}C derived chronologies and also demonstrates that exposure to KOH did not contaminate the geochemical signal. Williams (2009) also noted that exposure to KOH did not alter the stable isotope (carbon and nitrogen) signatures. Thus, delaminating the samples with KOH remains a reliable and effective approach to subsampling black corals (*Leiopathes* sp.) at high resolution (<200 µm).

Reservoir age-corrected ^{14}C ages suggested that deep-sea black corals in this region have grown continuously for at least the past 2 millennia (Fig. 6). These results are consistent with previous work illustrating that black corals exhibit extreme longevities (Roark et al. 2009). As mentioned earlier, previous age dating of black corals in the Gulf of Mexico focused on extrapolated ages and growth rates based on skeletal ^{210}Pb dating from limited samples (Williams et al. 2006, 2007). According to these prior studies, their sample from Viosca Knoll yielded a life span of 386 yr with an extrapolated growth rate of 14.5 µm yr^{-1}. This sample was collected alive, and therefore, its skeletal growth extended into the early 17th century (Williams 2009). Results from our current study greatly expand the age and growth rate distribution of deep-sea black corals from the Gulf of Mexico. The difference in the results between the 2 studies reflects the temporal coverage of the 2 dating methods as well as the application of measured ages rather than extrapolated ages. Only the last ~200 yr can be fully resolved by ^{210}Pb dating, beyond which growth rates and life span calculations have to be extrapolated. In contrast, radiocarbon dating is capable of dating specimens over the last ~50 000 yr with uncertainties ranging from approximately ± 20 to 400 yr or greater depending on the age of the specimen. Thus, choosing the appropriate dating technique capable of resolving the time period in question is critical to obtaining accurate and precise age and growth rates.

Growth rates

Long-term radial growth rates were calculated on black corals collected from the Gulf of Mexico, yielding growth rates ranging between 8 and 22 µm yr^{-1}. These results are consistent with growth rates from *Leiopathes* sp. specimens from Hawaii (Roark et al. 2009), and clearly confirm that *Leiopathes* sp. are the slowest-growing deep-sea corals relative to growth rates of other species. For example, the antipatharian *Stauropathes arctica* collected off Newfoundland yielded growth rates of 33 to 66 µm yr^{-1} (Sherwood & Edinger 2009). In comparison, growth rates measured

in bamboo corals off California were estimated at 50 to 110 µm yr^{-1} (Andrews et al. 2005), 50 to 60 µm yr^{-1} from the Gulf of Alaska (Roark et al. 2005), and 180 µm yr^{-1} from New Zealand (Tracey et al. 2007). *Gerardia* sp. from Hawaii, with average life spans of 950 yr (n = 23), yielded an overall average radial growth of 41 µm yr^{-1} (Parrish & Roark 2009), while Druffel et al. (1995) measured growth rates in *Gerardia* sp. from the Straits of Florida that were more consistent with *Leiopathes* sp. growth rates, ~5 µm yr^{-1} (Roark et al. 2009). This information is essential for assessing the vulnerability of these organisms to both natural and anthropogenic perturbations.

In most cases, radial growth rates were linear, except in 1 specimen (GOM-TOW-BC1) where the linear-age model yielded approximately 30% of the samples outside the age error window (Fig. 4e). The lack of pattern in these outliers suggested no contamination or influx of older ^{14}C, and replicate radiocarbon analyses did not indicate sampling contamination. This variance could represent natural ^{14}C variation (Druffel et al. 2008), which was possibly not captured in the other samples from the same location (GOM-TOW-BC2), due to a lower sample resolution (950 versus 220 µm increments). These variations are most likely related to changes in atmospheric ^{14}C concentration that are only captured at relatively high sampling resolution for ^{14}C analysis. Changes in the ^{14}C production rate due to solar variability are believed to be the major causal factor for the atmospheric $\Delta^{14}C$ variations during the Little Ice Age (LIA; Stuiver & Quay 1980, Bard et al. 1997). Atmospheric ^{14}C variation derived from tree rings during the LIA (~1300 to 1850 AD) indicate $\Delta^{14}C$ variability with amplitudes of ~20 to 28‰ (Reimer et al. 2004). This is consistent with the range of $\Delta^{14}C$ variability observed in the GOM-TOW-BC1 record (Fig. 4f). To fully explore the idea that ^{14}C records in *Leiopathes* sp. can be used as a water mass tracer will require the development of independent chronologies (maybe growth band counts) as well as replication studies using higher sampling frequencies for radiocarbon analysis.

Earlier work with *Gerardia* sp. (Druffel et al. 1995) suggested that deep-sea corals exhibit high rates of growth early in life. Likewise, Roark et al. (2009) also found faster radial growth rates over the initial 400 yr of a 2370 yr old *Leiopathes* sp. from Hawaii. While results from our study did not indicate faster initial growth rates within individual specimens, as concluded from calculating linear growth rates (R^2 values between 0.85 and 0.97), there is evidence of an inverse relationship between age (defined as life span) and growth rate at both sites (Fig. 6). Based on this relationship, growth rates decreased as the life span of the coral increased. For example, the growth rate of the oldest specimen, GOM-JSL04-4734-BC1, during the first 600 yr was 16 µm yr^{-1} (R^2 = 0.67), which is similar to the growth rate measured in GOM-JSL04-4734-BC1, which had a life span of 670 yr. Over the course of the specimen's life span, however, the average growth rate was slower, 8 µm yr^{-1} (R^2 = 0.87). Therefore, older specimens may be more vulnerable to disturbance as a result of slower average growth rates over the entire life span of the specimen. Given the extremely long life spans and very slow growth rates documented (even in the younger corals) in the Gulf of Mexico from our study and in the Pacific (Roark et al. 2006, 2009), it is unlikely that these species are renewable within the context of fishery management or even within a human life span. Any bottom-disturbing activity (e.g. bottom trawling, energy exploitation, anchoring) poses serious threats to these organisms. Given the proximity of these deep-sea coral sites, ~40 to 55 km north and northeast of the recent 'Deepwater Horizon' oil spill, and located under known surface slicks (http://response.restoration.noaa.gov/), these animals face additional threats that may require long-term monitoring to assess potential damage. Damage to black corals in the Gulf of Mexico will have long-term unresolved implications to the biodiversity in these deep-water reefs, requiring management efforts to protect sea floor habitats (National Marine Fisheries Service 2002).

Bomb signal

Given the reference bomb-^{14}C chronology derived from otolith and shallow coral $\Delta^{14}C$ records, bomb-^{14}C measurements in deep-sea black corals can be used to date these specimens (Roark et al. 2005, Sherwood et al. 2005, Sherwood & Edinger 2009). While the date of collection can be used to calculate life spans and growth rates for specimens collected alive, samples where the tissue layer has decayed and/or there is uncertainty as to whether the samples were collected alive (as with archived samples), an alternative approach is required. Therefore, as demonstrated in the present study, age models constructed from the rising and descending limbs of the bomb-curves can be used to reliably age date the outermost ring samples.

The outermost 1.25 mm layers of black coral contain bomb-derived carbon. The exception was the microdrilled GOM-TOW-BC2 sample, which yielded a $\Delta^{14}C$ value of −49 ± 33‰. This is in contrast to the outermost delaminated GOM-TOW-BC2 sample that yielded a $\Delta^{14}C$ value of 47 ± 18‰. Because the outermost microdrilled sample incorporates skeletal material over a distance of ~600 µm, the sample integrates over 75 yr of growth, including years in which no bomb carbon was produced. Thus, at sufficient sample resolution,

the proteinaceous skeleton from black corals can capture the surface-water $\Delta^{14}C$ history. The ability of the black corals to capture the surface-water $\Delta^{14}C$ history is a function of the animal's organic carbon source, i.e. surface-derived POM. If this were not the case, then the outer skeletal material would yield more depleted $\Delta^{14}C$ values. However, given the enriched $\Delta^{14}C$ values measured in the outer skeletal material (Table 4), there is no evidence indicating that the corals were feeding on old carbon. This is in contrast to coral calcite from bamboo corals, for example, where the carbonate material reflects the $\Delta^{14}C$ of the dissolved inorganic carbon (DIC) pool. For example, Roark et al. (2005) showed that coral calcite from a bamboo coral reflected seawater $\Delta^{14}C$ at ~700 m. The deep-sea coral record indicates a dramatic increase in $\Delta^{14}C$. Within a distance of 238 µm, $\Delta^{14}C$ values increased from −40 to 68‰. The 40‰ offset between the surface and deep-sea coral $\Delta^{14}C$ peak could reflect mixing with deep water, or more likely, that the subsampling resolution for ^{14}C analysis in the coral disc was not sufficient to capture the peak.

Radiocarbon time series from scleractinian corals provide information about surface and shallow circulation that can be used to test ocean dynamics in circulation models. For example, Grumet et al. (2005) conducted a model-data comparison using surface radiocarbon time series from coral records from the coasts of Kenya and Sumatra and a suite of dynamical 3-dimensional ocean models to test parameterizations of mixing and air–sea gas exchange between the ocean and atmosphere. The similarity of the $\Delta^{14}C$ history between the Flower Garden Banks shallow coral record and the deep-sea VK862 record (GOM-JSL04-4734-BC1) demonstrates that $\Delta^{14}C$ deep-sea coral records with independent chronologies can expand the temporal and spatial records used to document ocean $\Delta^{14}C$ variability.

CONCLUSIONS

Results from our study represent the first comprehensive investigation of growth rates and age distributions of black coral in the Gulf of Mexico and provide the qualitative background to assess negative impacts. Results from this work highlight the fact that these species in particular are the slowest-growing deep-sea corals and exhibit extreme longevities. Radiocarbon analysis of deep-sea black corals in the Gulf of Mexico indicated that these animals have been growing continuously for at least the last 2 millennia, with growth rates ranging from 8 to 22 µm yr^{-1}. Furthermore, the high degree of reproducibility found between discs, as well as within duplicate subsamples, validates the robustness of ^{14}C-derived chronologies. Reliable age models can be applied to multi-decadal paleoclimate reconstructions derived from the skeletal geochemistry. The presence of bomb-derived ^{14}C in the outermost ring samples of black coral skeletons confirms sinking POM as the dominant carbon source. The proximity of these communities to the 'Deepwater Horizon' oil spill may cause potential harm to these populations. Additionally, deprivation of surface-derived food sources could have adverse indirect effects on the deep-reef community given its dependence on sinking POM. We anticipate that the recovery of deep-sea corals, particularly black corals, would take at least decades to centuries. These reefs are unique ecological components of the Gulf of Mexico, and monitoring these unique reefs will provide scientific data that can be used to protect them.

Acknowledgements. The USGS Outer Continental Shelf Ecosystem Program and USGS Coastal and Marine Geology Program supported this work. We thank S. Griffin and E. Druffel (University of California, Irvine) and T. Guilderson (Lawrence Livermore National Laboratory) for assistance with radiocarbon analysis, and K. Sulak (USGS) and S. Cairns (Smithsonian Institution National Museum of Natural History) for donating samples, D. Opresko for species identification of some samples, and C. Holmes (USGS) for providing supplementary radiocarbon data. We also thank the entire USGS Diversity Systematic, and Connectivity of Valuable Reef Ecosystems (DISCOVRE) team for their support and collaboration. In addition, we are grateful to K. Sulak and T. Lorenson (USGS) for providing valuable editorial input as well as to several anonymous reviewers for their constructive comments and suggestions.

LITERATURE CITED

Abramoff MD, Magelhae PJ, Ram SJ (2004) Image processing with ImageJ. Biophotonics Int 11:36–42

Andrews AH, Cailliet GM, Kerr LA, Coale KH, Lundstrom C, DeVogelaere A (2005) Investigations of age and growth for three species of deep-sea coral from the Davidson Seamount off central California. In: Freiwald AJMR (ed) Cold-water corals and ecosystems. Springer-Verlag, Berlin, p 965–982

Baker MS, Wilson CA (2001) Use of bomb radiocarbon to validate otolith section ages of red snapper *Lutjanus campechanus* from the Northern Gulf of Mexico. Limnol Oceanogr 46:1819–1824

Bard E, Raisbeck GM, Yiou F, Jouzel J (1997) Solar modulation of cosmogenic nuclide production over the last millennium: comparison between ^{14}C and ^{10}Be records. Earth Planet Sci Lett 150:453–462

Becker EL, Cordes EE, Macko SA, Fisher CR (2009) Importance of seep primary production to *Lophelia pertusa* and associated fauna in the Gulf of Mexico. Deep-Sea Res I 56: 786–800

Broecker WS, Peng TS (1982) Tracers in the sea. Eldigio Press, Palisades, NY

Brooke S, Schroeder WW (2007) State of deep coral ecosystems in the Gulf of Mexico region: Texas to the Florida Straits. In: Lumsden SE, Hourigan TF, Bruckner AW Dorr

G (eds) The state of deep coral ecosystems of the United States. NOAA Tech Memo CRCP-3. Silver Spring, MD, p 271–306

Cordes EE, McGinley MP, Podowski EL, Becker EL, Lessard-Pilon S, Viada ST, Fisher CR (2008) Coral communities of the deep Gulf of Mexico. Deep-Sea Res I 55:777–787

CSA (Continental Shelf Associates) (2007) Characterization of northern Gulf of Mexico deepwater hard bottom communities with emphasis on *Lophelia* coral. In: US Department of Interior (ed) OCS Study MMS 2007-044. Minerals Management Service, Gulf of Mexico OCS Region, New Orleans, LA

Davies AJ, Duineveld GCA, van Weering TCE, Mienis F and others (2010) Short-term environmental variability in cold-water coral habitat at Viosca Knoll, Gulf of Mexico. Deep-Sea Res I 57:199–212

Druffel ERM, Griffin S, Witter A, Nelson E, Southon J, Kashgarian M, Vogel J (1995) *Gerardia*: bristlecone pine of the deep-sea? Geochim Cosmochim Acta 59:5031–5036

Druffel ERM, Robinson LF, Griffin S, Halley RB, Southon JR, Adkins JF (2008) Low reservoir ages for the surface ocean from mid-Holocene Florida corals. Paleoceanography 23: PA2209 doi:101029/2007PA001527

Duineveld GCA, Lavaleye MSS, Berghuis EM (2004) Particle flux and food supply to a seamount cold-water coral community (Galicia Bank, NW Spain). Mar Ecol Prog Ser 277: 13–23

Goldberg WM (1991) Chemistry and structure of skeletal growth rings in the black coral *Antipathes fiordensis* (Cnidaria, Antipathatia). Hydrobiologia 216-217:403–409

Goldberg W, Hopkins TL, Holl SM, Schaefer J, Kramer KJ, Morgan TD, Kim K (1994) Chemical composition of the sclerotized black coral skeleton (Coelenterata: Antipatharia): a comparison of two species. Comp Biochem Phys B 107:633–643

Grange KR (1985) Distribution, standing crop, population structure, and growth rates of black corals in the Southern fiord of New Zealand. N Z J Mar Freshw Res 19:467–475

Grange KR, Goldberg WM (1993) Chronology of black coral growth bands: 300 years of environmental history? In: Battershill CN, Schiel DR, Jones GP, Creese RG, MacDiamid AB (eds) Proc 2nd Int Temperate Reef Symp, Auckland, New Zealand. NIWA Marine, Wellington, p 169–174

Grigg RW (1965) Ecological studies on black coral in Hawaii. Pac Sci 19: 244–260

Grumet NS, Duffy PB, Wickett ME, Caldeira K, Dunbar RB (2005) Intrabasin comparison of surface radiocarbon levels in the Indian Ocean between coral records and three-dimensional global ocean models. Global Biogeochem Cycles 19: GB2010 doi:101029/2004GB002289

Hovland M (1990) Do carbonate reefs form due to fluid seepage? Terra Nova 2:8–18

Kim K, Goldberg WM, Taylor GT (1992) Architectural and mechanical properties of the black coral skeleton (Coelenterata: Antipatharia): a comparison of two species. Biol Bull (Woods Hole) 182:195–209

Kiriakoulakis K, Bett BJ, White M, Wolff GA (2004) Organic biogeochemistry of the Darwin Mounds, a deep-water coral ecosystem, of the NE Atlantic. Deep-Sea Res I 51: 1937–1954

Levin I, Kromer B (2004) The tropospheric $^{14}CO_2$ level in mid-latitudes of the Northern Hemisphere (1959–2003). Radiocarbon 46:1261–1272

Lewis JB (1978) Feeding mechanisms in black corals (Antipatharia). J Zool 186:393–396

Miller KJ (1997) Genetic structure of black coral populations in New Zealand's fiords. Mar Ecol Prog Ser 161:123–132

Miller KJ (1998) Short-distance dispersal of black coral larvae: inference from spatial analysis of colony genotypes. Mar Ecol Prog Ser 163:225–233

Miller K, Williams A, Rowden AA, Knowles C, Dunshea G (2010) Conflicting estimates of connectivity among deep-sea coral populations. PSZNI: Mar Ecol 31:144–157

National Marine Fisheries Service (NMFS-NOAA) (2002) Fisheries off west coast states and the western Pacific; precious corals fisheries; harvest quotas, definitions, size limits, gear restrictions, and bed classifications. Fed Regist 67: 11941–11945

Newton ED, Bak RPM (1979) Ecological aspects of Antipatharia (black corals) in Curaçao. Proc Assoc Isl Mar Lab Caribb 14:14

Nowak D, Florek M, Nowak J, Kwiatek W and others (2009) Morphology and the chemical make-up of the inorganic components of black corals. Mater Sci Eng C 29:1029–1038

Oakley SG (1988) Settlement and growth of *Antipathes pennacea* on a shipwreck. Coral Reefs 7:77–79

Opresko DM (2001) Revision of the Antipatharia (Cnidaria: Anthozoa). Part I: establishment of a new family, Myriopathidae. Zool Meded (Leiden) 75:147–174

Opresko DM (2002) Revision of the Antipatharia (Cnidaria: Anthozoa). Part II: Schizopathidae. Zool Meded (Leiden) 76:411–442

Opresko DM (2003) Revision of the Antipatharia (Cnidaria: Anthozoa). Part III: Cladopathidae. Zool Meded (Leiden) 77:495–536

Opresko DM (2004) Revision of the Antipatharia (Cnidaria: Anthozoa). Part IV: establishment of a new family, Aphanipathidae. Zool Meded (Leiden) 78:209–240

Parrish F, Roark E (2009) Growth validation of gold coral *Gerardia* sp. in the Hawaiian Archipelago. Mar Ecol Prog Ser 397:163–172

Parrish FA, Abernathy K, Marshall GJ, Buhleier BM (2002) Hawaiian monk seals (*Monachus schauinslandi*) foraging in deep-water coral beds. Mar Mamm Sci 18:244–258

Reimer PJ, Baillie MGL, Bard E, Bayliss A and others (2004) IntCal04 terrestrial radiocarbon age calibration, 0–26 cal kyr BP. Radiocarbon 46:1029–1058

Risk M, Heikoop J, Snow M, Beukens R (2002) Lifespans and growth patterns of two deep-sea corals: *Primnoa resedaeformis* and *Desmophyllum cristagalli*. Hydrobiologia 471: 125–131

Risk MJ, Sherwood OA, Nairn R, Gibbons C (2009) Tracking the record of sewage discharge off Jeddah, Saudi Arabia, since 1950, using stable isotope records from antipatharians. Mar Ecol Prog Ser 397:219–226

Roark EB, Guilderson TP, Flood-Page S, Dunbar RB, Ingram BL, Fallon SJ, McCulloch M (2005) Radiocarbon-based ages and growth rates of bamboo corals from the Gulf of Alaska. Geophys Res Lett 32:L04606 doi:10.1029/2004GL021919

Roark EB, Thomas PG, Robert BD, Ingram BL (2006) Radiocarbon-based ages and growth rates of Hawaiian deep-sea corals. Mar Ecol Prog Ser 327:1–14

Roark EB, Guilderson TP, Dunbar RB, Fallon SJ, Mucciarone DA (2009) Extreme longevity in proteinaceous deep-sea corals. Proc Natl Acad Sci USA 106:5204–5208

Roberts JM, Wheeler A, Freiwald A, Cairns S (2009) Cold-water corals: the biology and geology of deep-sea coral habitats. Cambridge University Press, Cambridge

Sánchez JA (1999) Black coral-octocoral distribution patterns on a deep-water reef, Imelda bank, Caribbean sea, Colombia. Bull Mar Sci 65:215–225

Schroeder WW, Brooke SD, Olson JB, Phaneuf B, McDonough JJ, Etnoyer P (2005) Occurrence of deep-water *Lophelia*

pertusa and *Madrepora oculata* in the Gulf of Mexico. In: Freiwald A, Roberts JM (eds) Cold-water corals and ecosystems. Springer-Verlag, Berlin, p 297–307

Sherwood O (2002) The deep-sea gorgonian coral *Primnoa resedaeformis* as an oceanographic monitor. MSc thesis, McMaster University, Hamilton, ON

Sherwood OA, Edinger EN (2009) Ages and growth rates of some deep-sea gorgonian and antipatharian corals of Newfoundland and Labrador. Can J Fish Aquat Sci 66: 142–152

Sherwood OA, Scott DB, Risk MJ, Guilderson TP (2005) Radiocarbon evidence for annual growth rings in the deep-sea octocoral *Primnoa resedaeformis*. Mar Ecol Prog Ser 301:129–134

Stuiver M, Polach HA (1977) Discussion: reporting of ^{14}C data. Radiocarbon 19:355–363

Stuiver M, Quay PD (1980) Changes in atmospheric carbon-14 attributed to a variable sun. Science 207:11–19

Stuiver M, Reimer PJ (1993) Extended ^{14}C database and revised CALIB radiocarbon calibration program. Radiocarbon 35:215–230

Sulak KJ, Brooks RA, Luke KE, Norem AD and others (2007) Demersal fishes associated with *Lophelia pertusa* coral and hard-substrate biotopes on the continental slope, northern Gulf of Mexico. In: George RY, Cairns SD (eds) Conservation and adaptive management of seamount and deep-sea coral ecosystems. University of Miami, Miami, FL, p 65–92

Sulak KJ, Randall MT, Luke KE, Norem AD, Miller JM (eds) (2008) Characterization of northern Gulf of Mexico deep-water hard bottom communities with emphasis on *Lophelia* coral—*Lophelia* reef megafaunal community structure, biotopes, genetics, microbial ecology, and geology. USGS Open-File Report 2008-1148; OCS Study MMS 2008-015. Available at http://fl.biology.usgs.gov/coastaleco/OFR_2008-1148_MMS_2008-015/index.html

Tracey MD, Neil H, Marriott P, Andrews HA, Cailliet MG, Sánchez JA (2007) Age and growth of two genera of deep-sea bamboo corals (family Isididae) in New Zealand waters. Bull Mar Sci 81:393–408

Wagner AJ (2009) Oxygen and carbon isotopes and coral growth in the Gulf of Mexico and Caribbean Sea as environmental and climate indicators. PhD thesis, Texas A&M University, College Station, TX

Wagner AJ, Guilderson TP, Slowey N, Cole JE (2009) Pre-bomb surface water radiocarbon of the Gulf of Mexico and Caribbean as recorded in hermatypic corals. Radiocarbon 51:947–954

Warner GF (1981) Species descriptions and ecological observations of black corals (Antipatharia) from Trinidad. Bull Mar Sci 31:147–163

Williams B (2009) Biogeochemistry of soft corals and black corals, and implication for paleoceanography in the western tropical Pacific. PhD thesis, The Ohio State University, Columbus, OH

Williams B, Risk MJ, Ross SW, Sulak KJ (2006) Deep-water antipatharians: proxies of environmental change. Geology 34:773–776

Williams B, Risk MJ, Ross SW, Sulak KJ (2007) Stable isotope data from deep-water antipatharians: 400-year records from the southeastern coast of the United States of America. Bull Mar Sci 81:437–447

Editorial responsibility: Charles Birkeland, Honolulu, Hawaii, USA

Submitted: October 11, 2010; Accepted: November 24, 2010
Proofs received from author(s): January 31, 2011